JOURNAL OF MATERIALS SCIENCE 29 (1994) 2328–2334

A study on the formation of liquation cracks in the weld heat-affected zone of HY-80 quenched and tempered steel

RONG-IUAN HSIEH, SHYI-CHIN WANG, HORNG-YIH LIOU
R & D Department, China Steel Corporation, Kaohsiung, Taiwan

Liquation cracking of heat-affected zones (HAZs) is often encountered during the welding of HY-80 steels. To reduce the sensitivity of this defect, the content of impurities, such as P and S, must be kept as low as possible. However, in the development of HY-80 steel, HAZ grain boundary liquation is still found even at very low impurity contents. In order to clarify the cause of this defect, the Gleeble hot ductility test and electron probe X-ray microanalysis (EPMA) were carried out. From the results of EPMA, it was evident that the grain boundary liquation in the heat-affected zone of HY-80 steel was due to the low-melting-point eutectic reaction between Cr, Ni and Mn, which had been swept up by the migrating grain boundaries in the welding–heating thermal cycle, and hence enriched at the grain boundary. In addition, the Gleeble hot ductility test results revealed that the HAZ liquation cracking sensitivity of HY-80 steel could be decreased by reducing the C, Ni and Cr contents of base metal, and by decreasing the dwell time at high temperatures during the welding thermal cycle.

1. Introduction

HY-80 steel is extensively used in the construction of warships and submarines owing to its high strength and superior low-temperature toughness. However, it is well known that liquation cracking of heat-affected zones (HAZs) is often encountered during welding of HY-80. The liquation cracking might contribute as an initiation site for cold cracking [1–4]. It is necessary to understand the mechanism for liquation crack formation so that precautions may be taken to eliminate this defect.

Liquation cracking, in contrast to other forms of cracking in the HAZ of ferritic steels, can be characterized by the following features [5].

1. The fracture propagation of this crack is always intergranular with respect to the prior austenite grain boundaries.
2. Liquation cracking is usually accompanied by an enrichment of some impurities or solutes at the prior austenite grain boundaries.
3. Liquation crack may vary in length from short microcracks confined to a part of a prior austenite grain boundary to microcracks a few grain diameters long.

Concerning the causes of HAZ liquation cracking of HY-80 steel, Masubuchi &Martin [1] have postulated that the sulphide inclusions in steels are responsible for the formation of this defect. However, Watanable & Okane [6] found that liquation in the prior austenite grain boundaries of HAZ was attributable to a melting reaction at low temperature, such as the eutectic reaction between Ni and Cr which segregated in grain boundaries. During the development of HY-80 steel, the HAZ liquation crack was also found in the HAZ even at a very low impurity contents. The purposes of this study are to clarify the cause of HAZ liquation cracking, to evaluate the effects of C, Cr, Ni elements on the HAZ liquation crack of HY-80 steel, and to investigate the effect of retention time at high temperature of the welding thermal cycle on the formation of HAZ liquation cracks.

2. Experimental procedure

Experimental steels were prepared from 250 kg vacuum-melted heats and cast into 160 × 160 mm square ingots. The chemical compositions of the experimental steels are listed in Table I. The contents of C, Cr and Ni ranged from 0.12–0.18, 1.0–1.27, and 2.0–2.55%, respectively. The P and S contents were kept at a very low level. Before rolling, the steels were reheated at 1200 °C for 2 h. During rolling the temperature was measured by an optical pyrometer, and the finish rolling temperature was around 920 °C; the plate thickness was 20 mm. After finish rolling, these steels were directly quenched in water and then tempered at 650 °C for 1 h. The mechanical properties and HAZ maximum hardness of experimental steels are listed in Table II; these all meet the specifications of HY-80 steel.

The specimens, with dimensions shown in Fig. 1, were prepared from the longitudinal direction of steel plates and subjected to HAZ thermal simulation using a Gleeble 1500 simulator to evaluate the liquation crack of HAZ. The hot ductility test was also carried

0022–2461

TABLE I Chemical compositions of experimental steels (wt %)

	C	Si	Mn	P*	S*	Al	Ni	Cr	Mo	Cu
Y1	0.15	0.19	0.30	80	44	0.01	2.54	1.26	0.25	0.11
Y2	0.15	0.18	0.29	90	45	0.01	2.44	0.95	0.23	–
Y3	0.12	0.19	0.30	90	46	0.01	2.55	1.27	0.25	–
Y4	0.18	0.19	0.30	90	49	0.01	2.55	1.27	0.25	–
Y5	0.15	0.19	0.31	90	42	0.03	2.00	1.02	0.23	–
Y6	0.12	0.18	0.29	90	42	0.03	2.01	1.04	0.23	–
Y7	0.18	0.18	0.30	90	42	0.03	2.02	1.03	0.23	–

* S, P in p.p.m.

TABLE II Mechanical properties of experimental steels

	YS ($kg\,mm^{-2}$)	TS ($kg\,mm^{-2}$)	EL (%)	– 18 °C (J)	– 85 °C (J)	HAZ Maximum microhardness
Y1	65.1	74.6	19.7	217	143	415
Y2	62.2	71.0	19.9	256	116	–
Y3	60.9	69.7	21.0	280	187	388
Y4	64.7	75.4	19.4	200	81	452
Y5	65.2	74.3	18.5	221	175	–
Y6	60.1	68.3	25.1	221	136	–
Y7	65.8	75.4	24.1	220	105	–

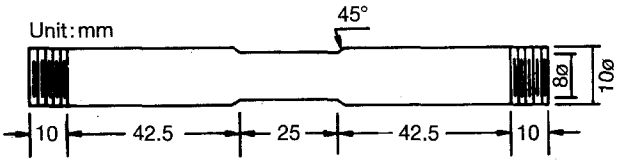

Figure 1 Dimensions of the Gleeble hot ductility test specimen.

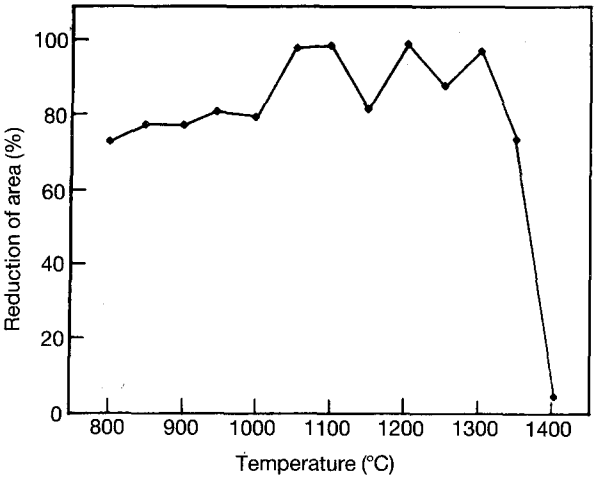

Figure 2 Relationship between temperature and reduction of area of Gleeble hot ductility test.

out at this Gleeble machine. In this test, the specimens were heated rapidly to 1400 °C and held for 1 and 5 s, and then cooled to the test temperature in the range between 800 and 1400 °C at a cooling rate of 1 °C s^{-1}. At the test temperature, the specimens were pulled to fracture at a tensile strain rate of 1.0 s^{-1}; the reduction in area was measured from these fractured specimens. The HAZ microstructure and fracture surface of the tensile specimen were examined using optical microscopy (OM) and scanning electron microscopy (SEM). At the same time, the electron probe microanalyser (EPMA) was also used to analyse the segregation and the distribution of certain alloy elements in the specimen.

3. Results and discussion

Fig. 2 shows the relationship between the temperature and the reduction of area of steel Y1 from the Gleeble hot ductility test. The hot ductility is superior when the test temperature is in the range from 800 to 1350 °C. However, the hot ductility decreased drastically when the test temperature was higher than 1350 °C. It has been reported that there are three temperature regions where the hot ductility trough is noticed in the carbon steels [7, 8], i.e. from melting point to 1200 °C (I), from 1200 to 900 °C (II) and from 900 to 600 °C (III). The mechanism of embrittlement in region I is the existence of a residual liquid film which is enriched with solute and impurities along the interdendritic interface. In region II, the precipitation of finely distributed oxy-sulphides at the austenite grain boundaries results in a deterioration of boundary cohesive strength. Furthermore, the embrittlement in region III is manifested by the precipitation of Nb (C, N) or AlN along the austenite grain boundaries [9, 10]. Based on the classification mentioned above, it may be assumed that the observed decrease in hot ductility of steel Y1 at temperatures over 1350 °C is related to the region I hot ductility trough, and results from partial liquation along the austenite grain boundaries.

Fig. 3 shows an SEM fractograph of the fracture surface of a hot ductility test specimen; the fracture surface is characterized by the intergranular fracture.

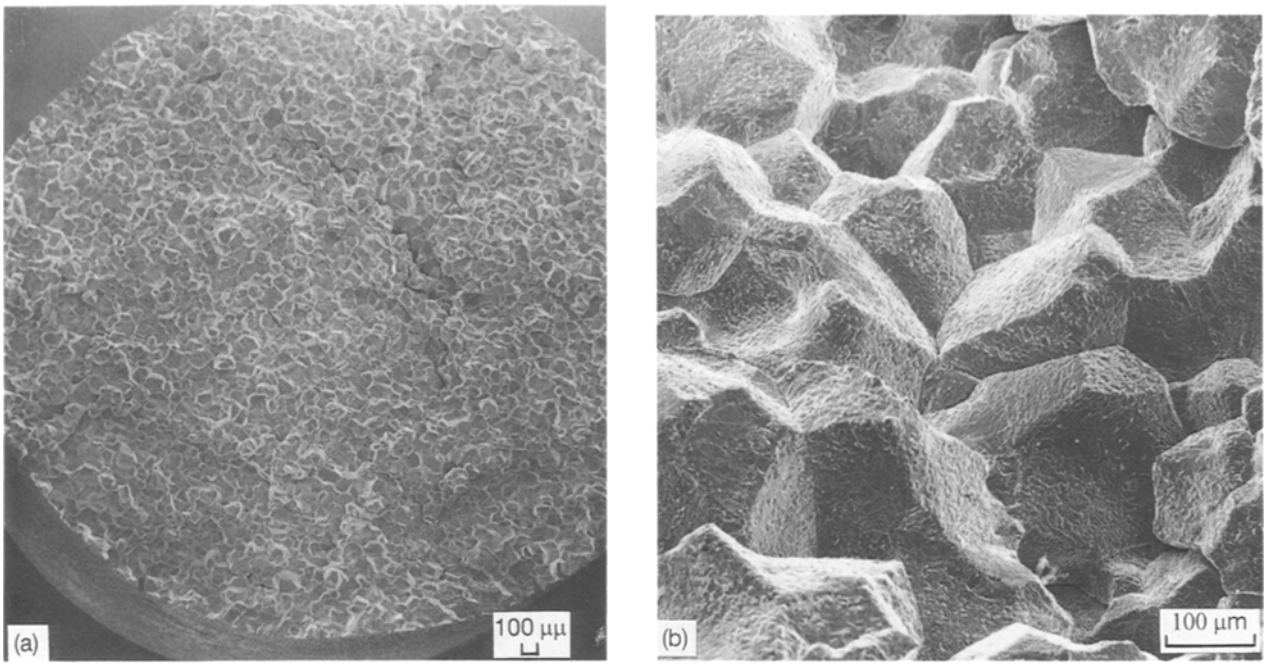

Figure 3 SEM fractograph of fracture surface of Gleeble hot ductility test specimen.

Figure 4 Microstructure of secondary crack beneath the main fracture surface.

At higher magnification, a secondary crack which is perpendicular to the main fracture surface can also be found. In order to observe the propagation feature of the secondary crack, a cross section which is longitudinal with respect to the specimen was taken, polished and etched. Fig. 4 shows the morphology of the secondary crack and its surrounding microstructures. It can clearly be seen that the crack propagated along a light-etching structure.

The element distribution profiles measured by EPMA along this light-etching structure are shown in Fig. 5. It can be seen that the Cr, Ni and Mn elements are enriched in this light-etching region. On the other hand, the element distribution profiles measured along a line beneath the secondary crack is shown in Fig. 6. It can be found that Cr is enriched to the left-hand side and depleted to the right-hand side of the secondary crack. However, the distribution of Ni is reversed. This result suggested that the path of this secondary crack is along the interphase boundary between the δ and γ phases of the solidification structure. In Fe-X binary phase diagrams, the maximum solubilities of Ni, Cr in δ-iron are 3.4 and 100%, respectively. The solubility of Cr in δ-iron is about 30 times higher than that of Ni. However, the solubilities of these elements in γ-iron are completely reversed: 100 and 12.5% for Ni and Cr, respectively [11]. Because of the significant difference in solubilities of Cr and Ni in δ-iron and γ-iron, the alloy partition in the vicinity of γ/δ phase boundary might occur. Fig. 7a shows the optical microstructure at a position beneath the main fracture surface of a fractured Gleeble specimen: a microcrack propagating along the prior austenite grain boundaries which has lighter contrast than that of the matrix can clearly be seen. From EPMA results (Fig. 7b–d) the enrichment of Mn, Ni and Cr elements at this light-etching austenite grain boundary can also be found.

To explore the cause of element enrichment at the austenite grain boundaries, the alloy distribution in the base metal was analysed by using EPMA. Fig. 8 shows the element line scanning analysis results in base metal. The segregation bands enriched in Cr, Ni and Mn exist periodically in the base metal. These segregation bands are thought to be inherited from the solute segregation zone located at interdendritic regions in the solidification structure of cast ingot. The solute segregation region is retained and flattened

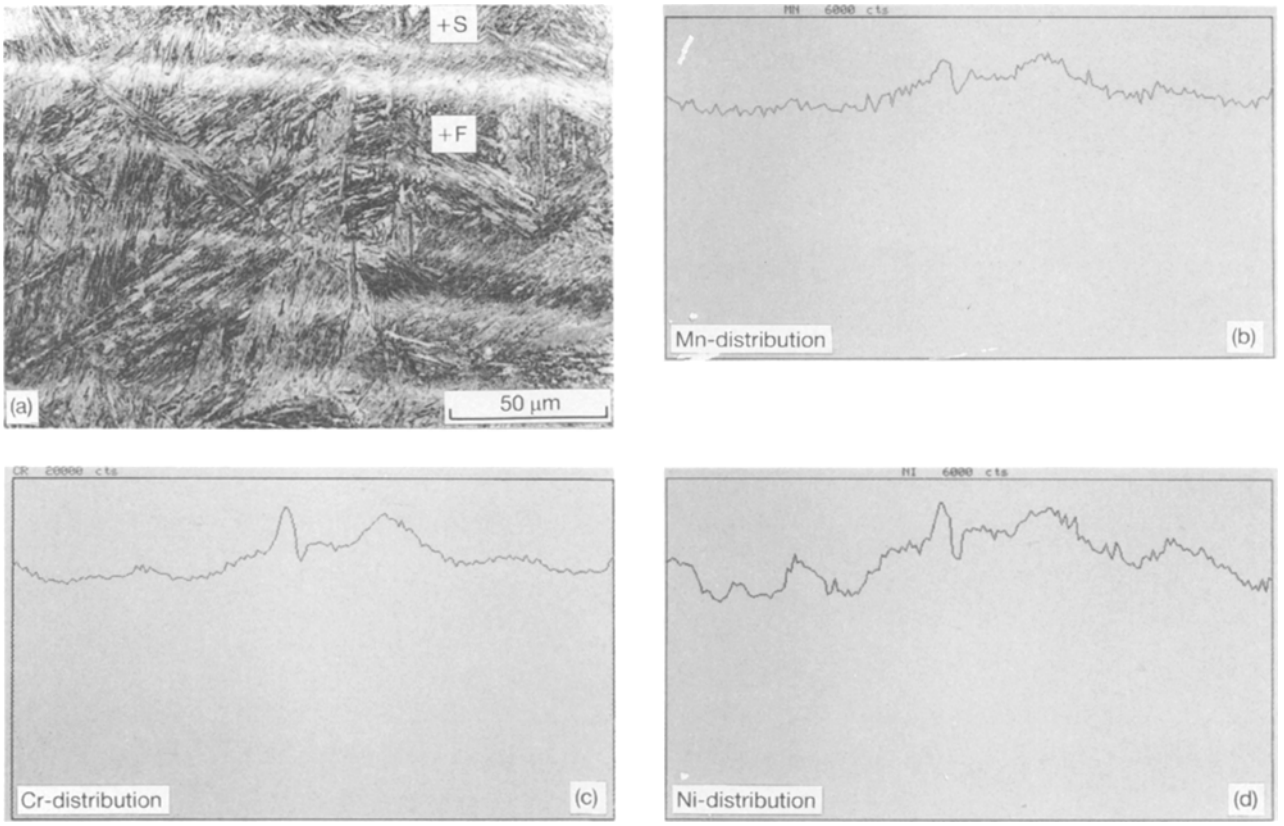

Figure 5 Microstructure and measured element distribution profiles in the vicinity of the heat-affected zone segregation band.

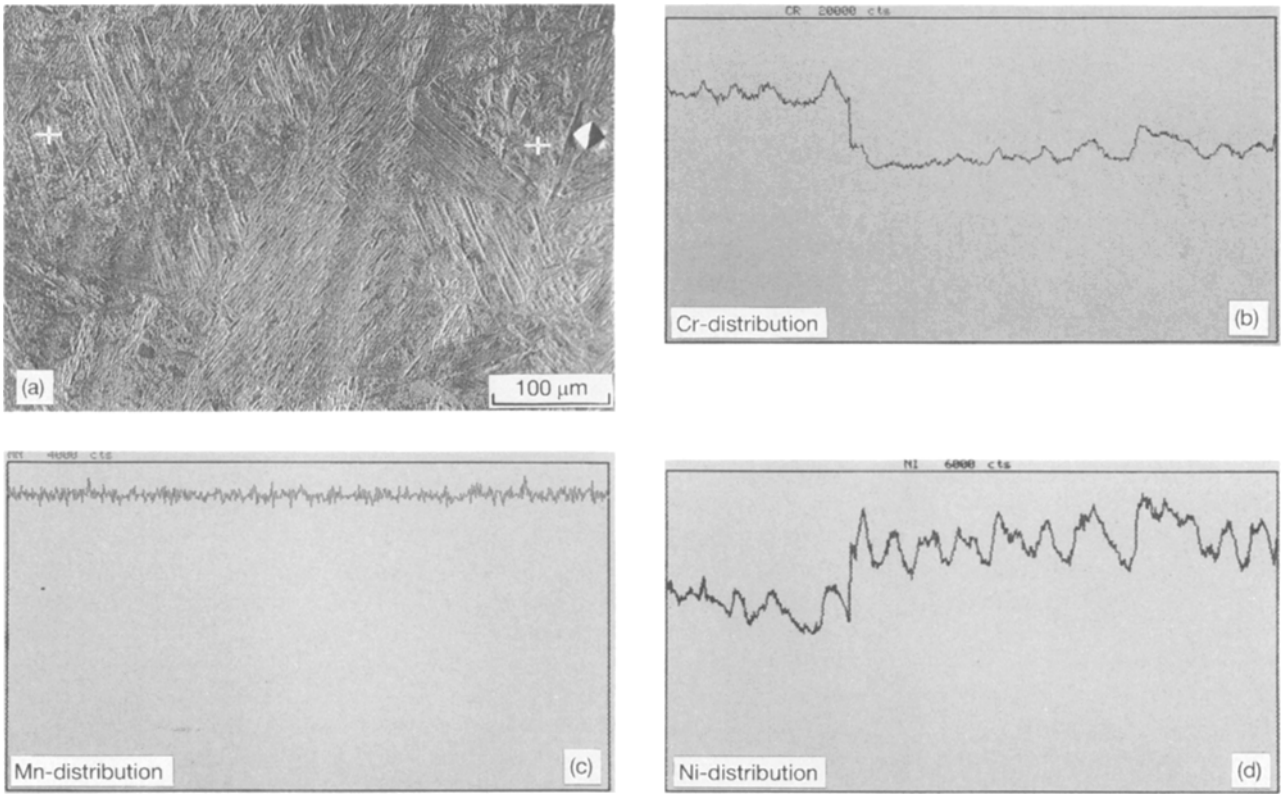

Figure 6 Optical micrograph and the measured alloy distribution profiles at position beneath the main fracture surface.

after rolling. Fig. 9 shows the measured segregation index as a function of the carbon content of steel. The segregation index is defined as X_{max}/X_{min}, which indicates a degree of segregation of elements at a band. The X_{max} and X_{min} are measured maximum and minimum alloy concentrations in the vicinity of a segregation band. It can be seen that the segregation index increases with increasing carbon content of the base metal.

Fig. 10 shows the evolution of solidification and microstructure as a result of the peritectic reaction

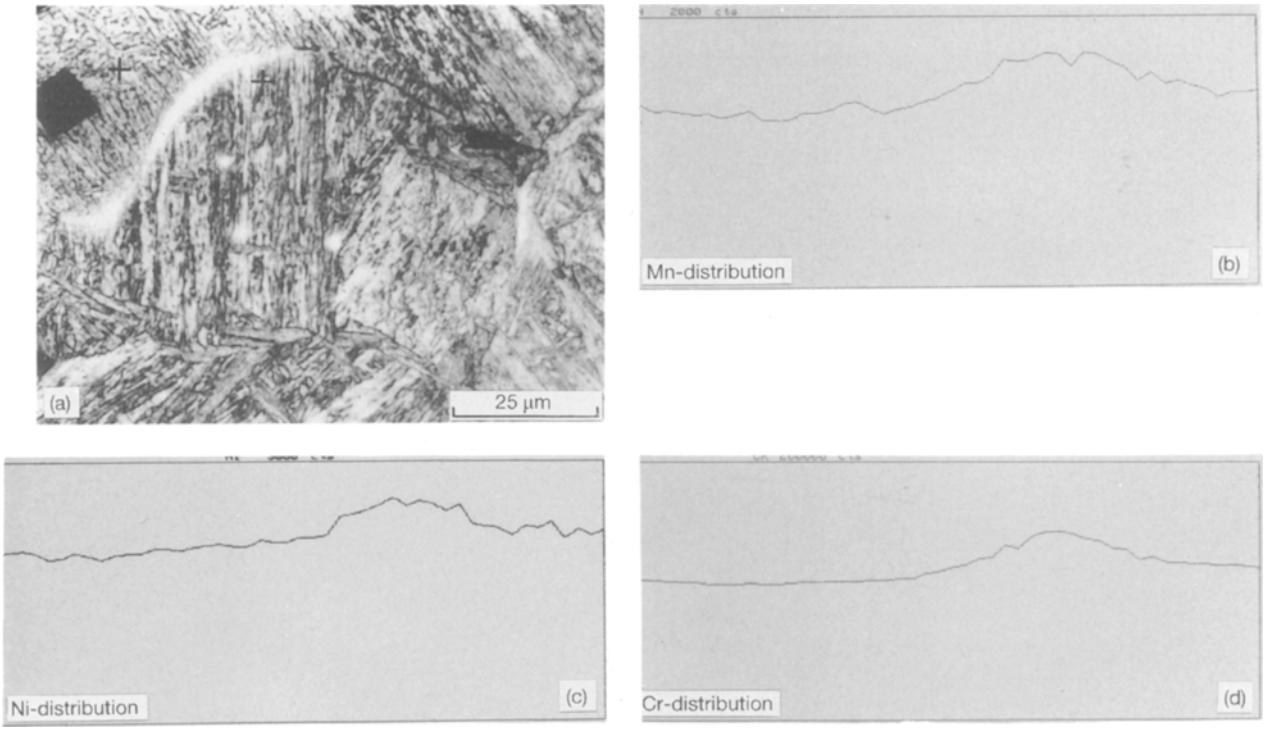

Figure 7 Optical micrograph of PAGB and the measured alloy distribution profiles at its vicinity.

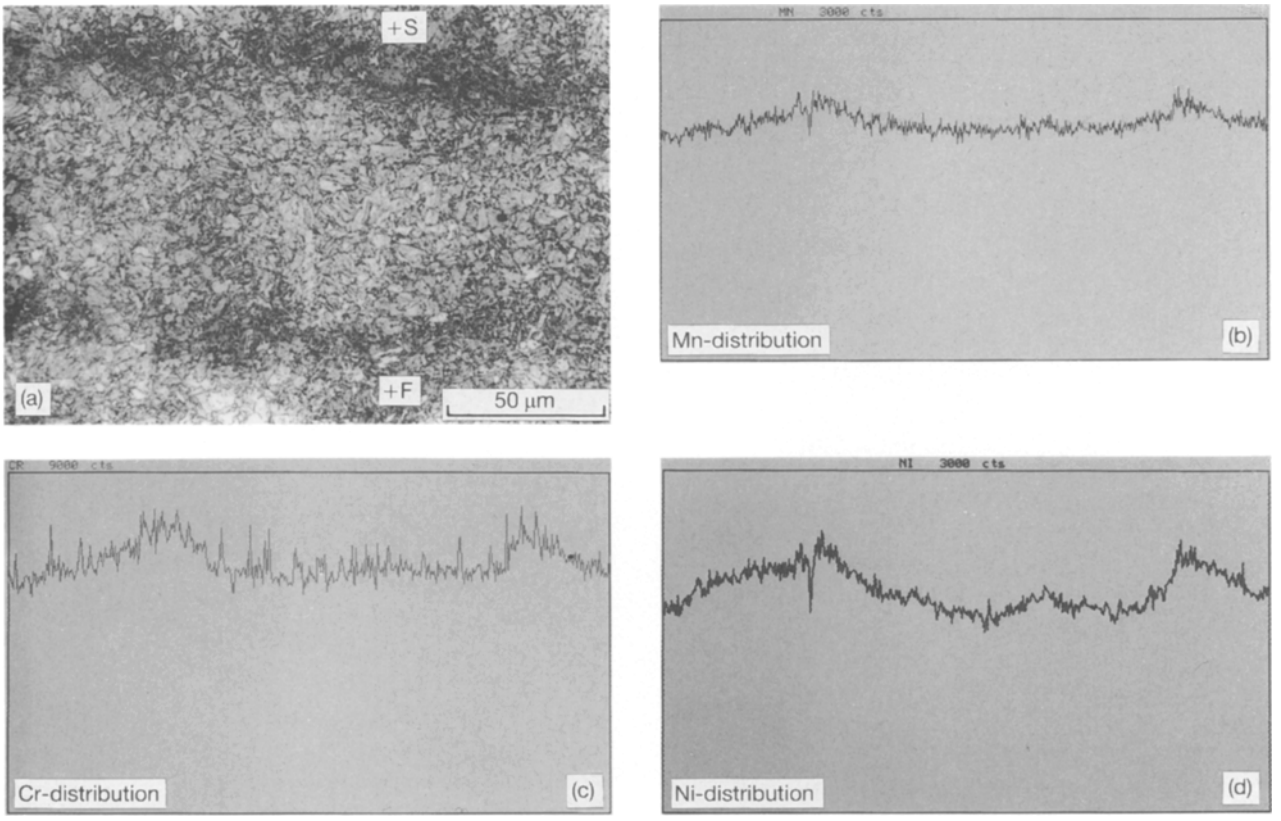

Figure 8 Optical micrograph of base metal and the measured alloy distribution profiles by EPMA.

extracting from the Fe–C phase diagram [12]. It is clear that the peritectic reaction and the accompanying γ-phase formation emerges earlier when the carbon content increases. It is well known that at the same temperature the diffusion rate of alloying element in the ferrite is hundreds of times higher than that in austenite, due to the difference in structure packing density [13]. Therefore, it can be proposed that if a peritectic reaction occurs, an austenite layer will form at the interface between pro-eutectic ferrite

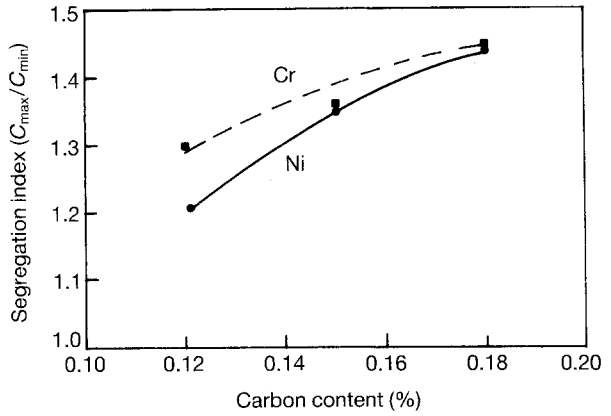

Figure 9 Variation of alloy segregation index with the carbon content in steels.

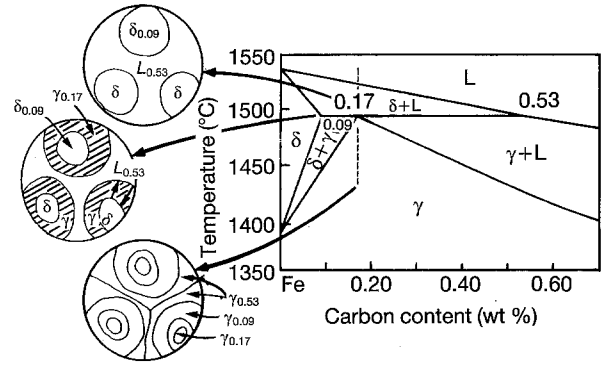

Figure 10 Evolution of solidification and microstructure as a result of peritectic reaction.

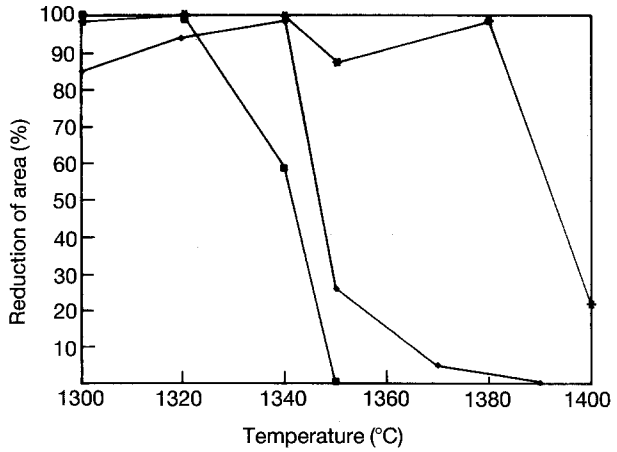

Figure 11 Variation of hot ductility with temperature for steels with different carbon contents. ✱, C 0.12%, Ni 2.54%, Cr 1.26%; ◆, C 0.15%, Ni 2.54%, Cr 1.26%; ■, C 0.18%, Ni 2.54%, Cr 1.26%.

and retained liquid, and the austenite layer behaves as a barrier to the transfer of alloy elements from alloy-enriched liquid to solid. As the solidification proceeds, the alloy content in the unsolidified liquid can be enriched up to the composition required for the eutectic reaction.

From the above results, it can be proposed that the mechanism to cause the grain boundaries liquation in the HAZ of HY-80 steel is due to the low-melting-point eutectic reaction between Cr, Ni and Mn which

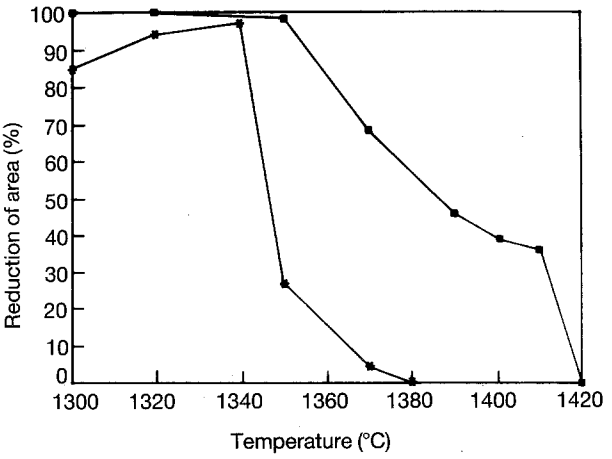

Figure 12 Variation of hot ductility with temperature for steels with different Ni and Cr contents. ✱, C 0.15%, Ni 2.54%, Cr 1.26%; ■, C 0.15%, Ni 2.0%, Cr 1.02%.

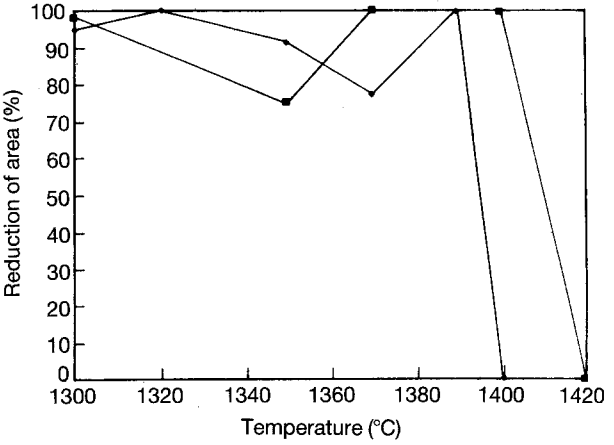

Figure 13 Variation of hot ductility with temperature for steels with soaking at 1400 °C for ■, 1s; ◆, 5s.

had been swept up by the migrating grain boundary in the process of the heating–welding thermal cycle. Because the S and P contents in the experimental steels were kept at a very low level in this study, the effect of these impurities on the HAZ liquation crack should be minor. According to the above analysis results, it is possible that the segregation tendency of alloy elements at the grain boundaries, and hence the liquation crack sensitivity of HAZ, might be reduced if the contents of C, Cr and Ni in the base metal can be decreased.

Fig. 11 shows the relationship between the carbon content and the hot ductility. The hot ductility increases significantly with decreasing carbon content of the base metal. Fig. 12 shows the variation of hot ductility with temperature for steels with different Cr and Ni content. The improvement of hot ductility with decreasing alloying contents is evident. Fig. 13 shows the effect of soaking time on the hot ductility. The hot ductility is deteriorated with increasing soaking time, probably due to the enrichment of alloying elements which results in a lower melting point at grain boundaries. Therefore, the liquated grain boundaries are formed in a wider area.

4. Conclusions

In the development of HY-80 steels, the HAZ grain boundary liquation crack was found even at very low impurity contents. From the results of EPMA and the Gleeble hot ductility test, the main conclusions were drawn as follows.

1. The most important factors causing grain boundary liquation in the heat-affected zone of HY-80 steel was due to the low-melting point eutectic reaction between Cr, Ni and Mn, which had been swept up by the migrating grain boundaries in the process of the heating–welding thermal cycle and hence enriched at the grain boundary.
2. The HAZ liquation cracking sensitivity of HY-80 steel could be decreased by reducing the C, Ni and Cr contents of base metal and decreasing the dwell time at high temperature during the welding thermal cycle.

References

1. K. MASUBUCHI and D. C. MARTIN, *Welding Journal* **41** (1962) 375S.
2. H. TAMURA and T. WATANABLE, *Journal of the Japan Welding Society* **42** (1973) 966.
3. T. WATANABLE, *Transactions of the Japan Welding Society* **19** (1988) 28.
4. W. F. SAVAGE, E. F. NIPPES and H. HOMMA, *W. J.* **55** (1976) 386.
5. T. BONISZEWSKI and R. G. BAKER, *JISI* **202** (1964) 921.
6. T. WATANABLE, I. OKANE, *Trans. J. W. S.* **13** (1982) 19.
7. H. FUJI, M. ODA, T. OHASHI and K. HIROMOTO, *Tetsu-to-Hagane* **62** (1976) S. 93.
8. S. HASEBE, T. KOGA, T. YAMURA and Y. SUJIKAWA, *ibid.* **58** (1972) S. 221.
9. H. G. SUZUKI, S. NISHIMURA and S. YAMAGUCHI, *ibid.* **65** (1979) 2038.
10. H. G. SUZUKI, S. NISHIMURA and S. YAMAGUCHI, *Trans. Iron & Steel Institute of Japan* **22** (1982) 48.
11. M. HANSEN, "Constitution of Binary Alloys" (McGraw-Hill, New York, 1958).
12. D. R. ASKELAND, "The Science and Engineering of Materials" 1st Edn (Brooks, Cole Engineering Division, 1984) p.259.
13. H. FREDRIKSSON, *Scand. J. Metall.* **5** (1976) 27.

Received 6 May
and accepted 6 October 1993